Phosphorylation of aquaporin-2 regulates its endocytosis and protein–protein interactions

Hanne B. Moeller, Jeppe Praetorius, Michael R. Rützler, and Robert A. Fenton

Water and Salt Research Center, Department of Anatomy, Aarhus University, DK-8000 Aarhus C, Denmark

Edited by Peter C. Agre, Johns Hopkins Malaria Research Institute, Baltimore, MD, and approved November 4, 2009 (received for review September 18, 2009)

The water channel aquaporin-2 (AQP2) is essential for urine concentration. Vasopressin regulates phosphorylation of AQP2 at four conserved serine residues at the COOH-terminal tail (S256, S261, S264, and S269). We used numerous stably transfected Madin–Darby canine kidney cell models, replacing serine residues with either alanine (A), which prevents phosphorylation, or aspartic acid (D), which mimics the charged state of phosphorylated AQP2, to address whether phosphorylation is involved in regulation of (*i*) apical plasma membrane abundance of AQP2, (*ii*) internalization of AQP2, (*iii*) AQP2 protein–protein interactions, and (*iv*) degradation of AQP2. Under control conditions, S256D- and 269D-AQP2 mutants had significantly greater apical plasma membrane abundance compared to wild type (WT)-AQP2. Activation of adenylate cyclase significantly increased the apical plasma membrane abundance of all S-A or S-D AQP2 mutants with the exception of 256D-AQP2, although 256A-, 261A-, and 269A-AQP2 mutants increased to a lesser extent than WT-AQP2. Biotin internalization assays and confocal microscopy demonstrated that the internalization of 256D- and 269D-AQP2 from the plasma membrane was slower than WT-AQP2. The slower internalization corresponded with reduced interaction of S256D- and 269D-AQP2 with several proteins involved in endocytosis, including Hsp70, Hsc70, dynamin, and clathrin heavy chain. The mutants with the slowest rate of internalization, 256D- and 269D-AQP2, had a greater protein half-life ($t_{1/2}$ = 5.1 h and $t_{1/2}$ = 4.4 h, respectively) compared to WT-AQP2 ($t_{1/2}$ = 2.9 h). Our results suggest that vasopressin-mediated membrane accumulation of AQP2 can be controlled via regulated exocytosis and endocytosis in a process that is dependent on COOH terminal phosphorylation and subsequent protein–protein interactions.

Madin–Darby canine kidney cells | trafficking | vasopressin | water homeostasis | water channel

Aquaporin-2 (AQP2) is a water-channel protein expressed in the collecting duct of the kidney. Following increased vasopressin (AVP) levels, shuttling and fusion of AQP2 vesicles to the apical plasma membrane lead to water absorption and urine concentration. Knepper and Nielsen proposed that the plasma membrane abundance of AQP2 is a regulated balance between endocytosis and exocytosis (1). The downstream effects of the AVP-mediated signaling cascade on AQP2 exocytosis are complex and involve activation of adenylate cyclase, increased cAMP and intracellular Ca^{2+} levels, and increased protein kinase A (PKA) activation. Additionally, both nitric oxide and atrial naturetic peptide, known to increase cGMP levels, can induce apical AQP2 accumulation (2). Currently, little is known about the process of AQP2 endocytosis, although it has been reported that both prostaglandin E2 and dopamine can induce AQP2 internalization (3) and that AQP2 ubiquitination is also involved (4).

AVP regulates the phosphorylation of four residues in the carboxyl terminal tail of AQP2 at positions S256, S261, S264, and S269 (5–7). S256 phosphorylation is critical for AQP2 trafficking in a number of studies (8, 9). Recent studies suggest that S261 is not required for AQP2 trafficking (10). The precise roles of the other phosphorylation sites remain unclear, although different "phosphoforms" have distinct cellular localizations and have been proposed to be involved in regulating endocytosis and protein degradation (6, 7, 11). Polyphosphorylation of AQP2 does not affect the relative unit water permeability of the channel (12), so it is unlikely to be involved in channel gating. Another hypothesis is that phosphorylation can influence AQP2 interactions with proteins involved in exocytosis or endocytosis (13), and several proteins have been identified that bind to AQP2, including Hsp70, Hsc70, clathrin, dynamin, AP2 (14), MAL (15), Spa-1 (16), lip 5 (17), annexin (18), Hsp50-5(BiP/Grp78), and PP1 (13).

In this study, we comprehensively examine the role of the polyphosphorylation of AQP2. We show that phosphorylation can alter the extent of both AQP2 exocytosis and AQP2 endocytosis. The rate of AQP2 endocytosis is influenced by phosphorylation at S256 and/or S269, and this is concurrent with altered protein–protein interactions with the endocytic machinery. Additionally, we demonstrate that phosphorylation can influence cellular AQP2 abundance via regulation of protein degradation.

Results

Mutation of Phosphorylation Sites in the COOH Terminal Tail of AQP2 Alters Its Cellular Distribution. The localization of various phosphorylation-deficient (Ser to Ala) or "constitutively phosphorylated" (Ser to Asp) AQP2 mutants either under control conditions or in response to forskolin treatment was examined by immunocytochemistry. Representative images are shown in Fig. 1. Wild type (WT)-AQP2 is observed predominantly in intracellular compartments in control (nonstimulated) conditions and accumulates in the apical plasma membrane in response to forskolin. Similarly, under control conditions the mutants 261A-AQP2, 261D-AQP2, 264A-AQP2, and 264D-AQP2 reside in intracellular vesicles and accumulate in the plasma membrane in response to forskolin. In contrast, 256D-AQP2 and 269D-AQP2 are predominantly located in the plasma membrane in control conditions, whereas 256A-AQP2 is predominantly located in intracellular compartments even after treatment with forskolin. To confirm these observations and quantify AQP2 membrane abundance in each of the cell lines, we performed a cell-surface biotinylation assay under control conditions or after 30 min of forskolin treatment (Fig. 2). In all cell lines, with the exception of AQP2-256D-expressing cells, membrane abundance of AQP2 increased significantly in response to forskolin (Fig. 2*B*). In comparison with WT-AQP2-expressing cells, the apical membrane abundance of AQP2 under control conditions was significantly higher in the 256D-AQP2 and 269D-AQP2 cell lines (Fig. 2*C*), whereas the relative abundance on the membrane after forskolin treatment was not significantly

Author contributions: H.B.M., J.P., M.R.R., and R.A.F. designed research; H.B.M., J.P., and R.A.F. performed research; H.B.M., J.P., M.R.R., and R.A.F. analyzed data; and H.B.M. and R.A.F. wrote the paper.

The authors declare no conflict of interest.

This article is a PNAS Direct Submission.

To whom correspondence should be addressed at: The Water and Salt Research Center, Department of Anatomy, Wilhelm Meyers Alle, Aarhus University, DK-8000 Aarhus, Denmark. E-mail: rofe@ana.au.dk.

This article contains supporting information online at www.pnas.org/cgi/content/full/0910683107/DCSupplemental.

www.pnas.org/cgi/doi/10.1073/pnas.0910683107

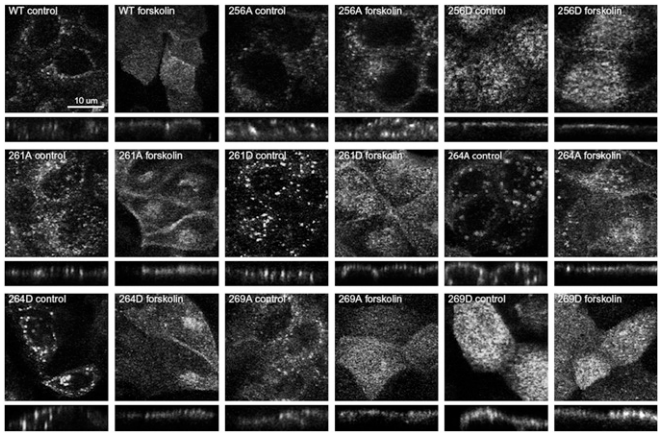

Fig. 1. Trafficking of AQP2 in MDCK cells expressing various forms of mutated AQP2. Representative confocal laser scanning images are shown in both X–Y and X–Z projections.

different. In contrast, the relative membrane abundance of AQP2 after forskolin treatment was significantly less in 256A-AQP2–, 261A-AQP2–, and 269A-AQP2–expressing cells.

Mutation of Phosphorylation Sites in the COOH Terminal Tail of AQP2 Alters Internalization of the Protein. The relative differences in AQP2 membrane abundances could be due to differences in AQP2 trafficking to the membrane or AQP2 retrieval from the membrane. To examine whether differences in AQP2 internalization rates exist among the mutated forms of AQP2, we performed a protein internalization assay (Fig. 3). Cells, either control or forskolin stimulated, were biotinylated at 4°C from the apical side and reincubated at 37°C for various time points to allow biotinylated proteins to internalize. Biotin was subsequently stripped from the apical cell surface, leaving only internalized AQP2 biotinylated. These fractions were assessed by immunoblotting (Fig. 3*A*). Data from all cell lines are summarized in Fig. S1. Compared to WT-AQP2, 256D-AQP2 and 269D-AQP2 were internalized at a significantly reduced rate (Fig. 3*B*). Additionally, 269D-AQP2 was internalized significantly less than 269A-AQP2 after 20, 40, and 80 min. No significant differences were observed in the degree of internalization of the other AQP2 mutants compared to WT-AQP2 (Fig. S1).

To visualize the cellular distribution of biotin and AQP2 during the internalization assay and assess the validity of our biochemical data, we performed immunocytochemistry on WT-AQP2, 269A-AQP2, and 269D-AQP2 cells treated under similar conditions. Representative images of the cell lines at various time points are shown in Fig. 4. Biotin, depicted in red, has a clear apical plasma membrane distribution in control and forskolin-treated cells, demonstrating that, under our experimental conditions, biotin itself does not cross the cell membrane. At time point 0, the 2-mercaptoethane sulfonate sodium (MesNa)-based stripping of apical biotin reduced the labeling of the plasma membrane considerably. After reincubation of the cells at 37°C (20 and 40 min of washout), biotin labeling was distinctly intracellular and punctuate in appearance. The distribution of AQP2 (depicted in green in Fig. 4) in all three cell lines under control and forskolin-stimulated conditions was as described earlier (Fig. 1). WT-AQP2 and the mutant forms 269A-AQP2 and 269D-AQP2 are internalized in response to forskolin washout, with AQP2-269D having a prolonged apical plasma membrane distribution consistent with the biochemical data. In all cell lines, a proportion of AQP2 that has been biotinylated in the apical plasma membrane and subsequently internalized colocalizes with biotin in endocytosed vesicles. Biotin-positive and AQP2-negative vesicles are also observed, corresponding to the endocytosis of other proteins from the plasma membrane or, alternatively, to AQP2-containing vesicles that were not initially transported to the cell surface following stimulation.

Mutation of Phosphorylation Sites in the COOH Terminal Tail of AQP2 Alters AQP2 Protein–Protein Interactions. The altered membrane abundances and different internalization rates observed for 256D- and 269D-AQP2 potentially could be explained by differences in AQP2 protein–protein interactions. To examine this, we performed AQP2 co-immunoprecipitation on cells under control or forskolin-stimulated conditions, followed by immunoblotting for proteins known to interact with AQP2 and to regulate the trafficking and sorting of proteins (see Table S1). The results are summarized in Fig. 5. γ-Actin had a greater interaction with 256A-AQP2 than all other mutants in both the presence and the absence of forskolin. Furthermore, the interaction of γ-actin with WT-AQP2 was reduced after forskolin stimulation, suggesting that γ-actin is released from AQP2 following phosphorylation. Both annexin-2, a Ca^{2+}-dependent effector protein that can function as an organizer of membrane domains (19), and protein phosphatase 1 were significantly more abundant in pull-downs from 256A-AQP2-expressing cells compared to WT-AQP2 cells. These findings are in line with previous observations showing that both proteins bind preferentially to a nonphosphorylated S256 AQP2 peptide (13). Additionally, we observed significantly reduced annexin-2 binding to WT-AQP2 following forskolin treatment, presumably due to an increased fraction of AQP2 phosphorylated at S256. Both Hsp70 and Hsc70 have been shown to interact with AQP2 and possibly contribute to clathrin-mediated endocytosis (14). In our studies, Hsp70 bound significantly less to 269D-AQP2 compared to WT-AQP2. Furthermore, there was a reduced interaction between Hsc70 and 256D-AQP2 and 269D-AQP2, along with an increased interaction with 269A-AQP2. Two other proteins involved in endocytic processes that co-immunoprecipitate (co-IP) with AQP2 (14), clathrin heavy chain and dynamin, were also significantly lower in abundance in pull-downs from 256D-AQP2 and 269D-AQP2 cell lines compared to AQP2-WT, irrespective of forskolin treatment. Taken together, these observations support our hypothesis that the 256/269D-substituted forms of AQP2, mimicking phosphorylation at these sites, are predominantly detected on the plasma membrane due to decreased endocytosis. Despite repeated attempts, and using different antibodies, we were unable to pull down the previously reported AQP2-interacting proteins—SPA-1, MAL, or tropomyosin 5b—from our Madin–Darby canine kidney (MDCK) cells.

AQP2 Protein Degradation Is Altered by Mutations in the COOH Terminal Tail of AQP2. One way to regulate total protein abundance is to regulate the protein degradation rate. Membrane-associated proteins must be internalized to enter the cell degradation pathways. A reduced rate of endocytosis, as observed for 256D-AQP2 and 269D-AQP2, could therefore increase the protein half-life of these forms of AQP2. To address this possibility, we examined AQP2 degradation in each of the MDCK cell lines. Protein synthesis was blocked with cycloheximide, following which protein samples were prepared at various time points and subjected to immunoblotting for AQP2. Results are summarized in Fig. 6. (see Fig. S2 for results from all cell lines). The calculated half-life of WT-AQP2 was 2.9 h. Substitution of serine residues at 261 with either alanine or aspartic acid resulted in AQP2 half-lives of 2.6 and 2.4 h, respectively, whereas 264D-AQP2 had a slightly longer half-life of 3.8 h. The shortest half-life of 1.6 h was observed for 256A-AQP2. 256D-AQP2- and 269D-AQP2-expressing cells, which had the slowest rate of AQP2 internalization, had the longest AQP2 half-lifes of 5.1 and 4.4 h, respectively. Indeed, even after long-term cycloheximide

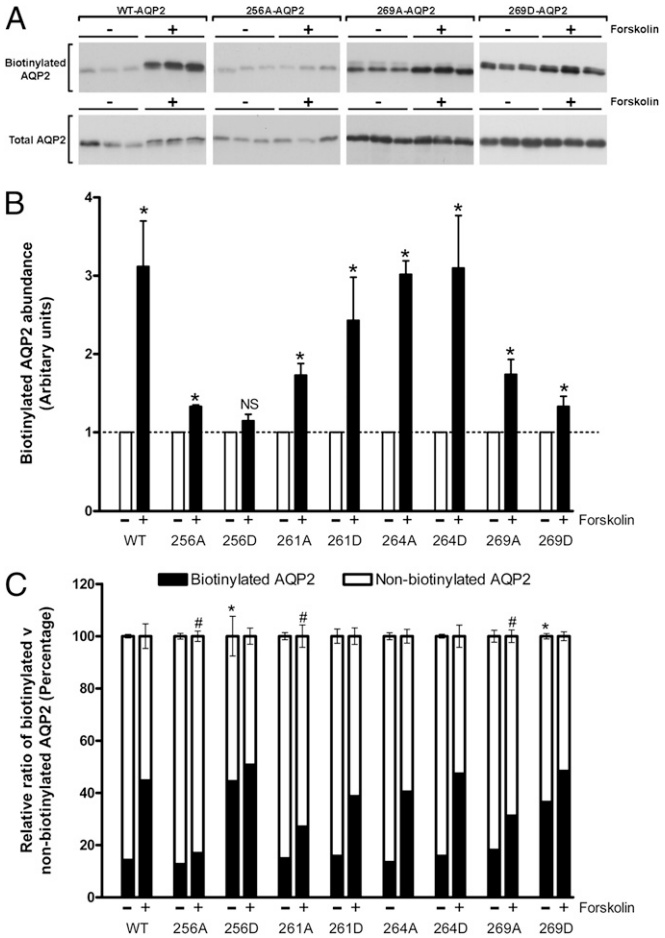

Fig. 2. Cell-surface biotinylation assay of MDCK cells expressing various forms of mutated AQP2. (*A*) Representative immunoblots of biotinylated versus total AQP2. (*B*) Relative AQP2 membrane abundance after forskolin treatment compared to control conditions. (*C*) Relative quantification of biotinylated and nonbiotinylated AQP2 fractions. An asterisk indicates a significant difference compared to WT-AQP2 in control conditions. "#" indicates a significant difference compared to WT-AQP2 after forskolin treatment.

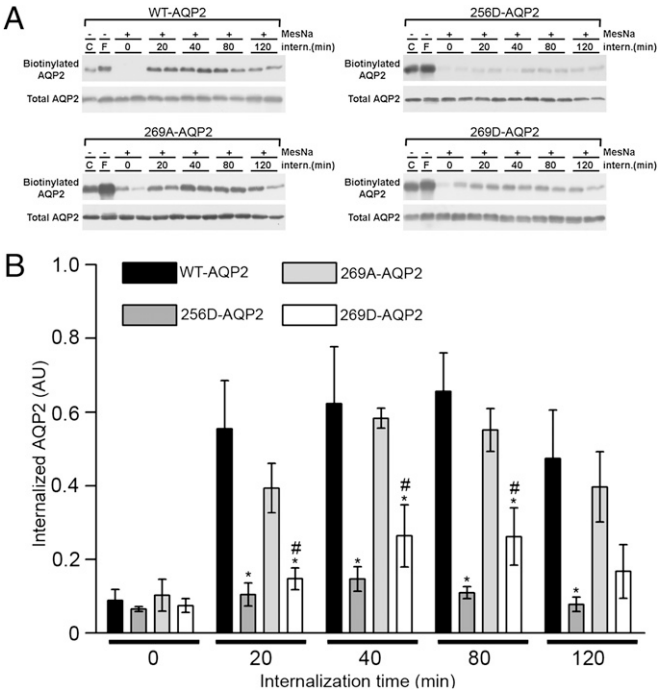

Fig. 3. Internalization of mutated AQP2 accessed by biotin internalization assay. (*A*) Representative immunoblots are shown for illustration. C, control condition; F, forskolin. (*B*) A comparison of internalization for the cell lines WT-AQP2, AQP2-256A, AQP2-269A, and AQP2-269A. An asterisk indicates a significant difference compared to WT-AQP2. "#" indicates a significant difference of D-substituted mutants compared to corresponding A substitutions.

treatment (Fig. S3), both S256D and S269D forms of AQP2 were relatively abundant.

Discussion

The total abundance of AQP2 on the plasma membrane has been suggested to be a regulated balance between endocytosis and exocytosis (1, 20). Constitutive trafficking of AQP2 to and from the plasma membrane occurs continuously, even in the absence of AVP or when S256 of AQP2 is replaced by the amino acid alanine that cannot be phosphorylated (8, 21, 22). In contrast, membrane trafficking processes that control the abundance of AQP2 in the membrane in response to AVP depend on the phosphorylation of AQP2 at S256 (3, 23). S256 is part of a "polyphosphorylated" region containing four AVP-regulated phosphorylation sites (S256, S261, S264, and S269) within the last 16 amino acids of the AQP2 COOH-terminal tail (24). In the present study, we used MDCK cell models to demonstrate that COOH-terminal phosphorylation is critical for AQP2 exocytosis, endocytosis, and protein degradation (see Fig. S4 for our scheme of AQP2 trafficking based on this study and previous knowledge). We conclude that phosphorylation of both S256 and S269 can result in increased AQP2 abundance on the plasma membrane due to reduced internalization of the channel, a process that is concurrent with reduced protein–protein interactions with the endocytic machinery. In the following, we expand on these conclusions in the context of current knowledge regarding AQP2 regulation.

Phosphorylation of AQP2 Regulates Both Its Endocytosis and Its Exocytosis. PKA-induced phosphorylation of AQP2 at S256 is necessary for membrane accumulation of AQP2 in response to AVP (8, 9), which is thought to occur predominantly through pS256-induced AQP2 trafficking. Indeed, our results confirm several other studies (3, 9, 23) showing that 256A-AQP2, which cannot be phosphorylated at this residue, is predominantly localized to intracellular vesicles, suggesting a role of S256 in AQP2 exocytosis. In contrast, 269A-AQP2 retains the ability to accumulate on the membrane in response to forskolin stimulation, suggesting that S269 phosphorylation is not necessary for AQP2 exocytosis. Despite these apparent differences between 256A- and 269A-AQP2-expressing cells, mutating AQP2 to replace either S256 or S269 with an aspartate (creating a fixed negative charge mimicking a phosphoserine) resulted in AQP2 localization predominantly in the plasma membrane, even without measures to increase intracellular cAMP. These results suggest that whereas only S256 is necessary for AQP2 exocytosis, phosphorylation of both S256 and S269 can modulate AQP2 endocytosis. Indeed, the results from our cell models fit well with in vivo localization studies demonstrating that pS256-AQP2 is distributed throughout the cell but increases on the plasma membrane following AVP stimulation, whereas pS269-AQP2 is detected only in the apical plasma membrane (7, 11).

Our studies demonstrate that both S261A and S261D mutated forms of AQP2 are able to accumulate on the plasma membrane in response to forskolin stimulation. These results are in line with our previous observations that S261 phosphorylation is independent of S256 phosphorylation (12) and studies from Lu et al. indicating that S261 is not required for either AVP-stimulated

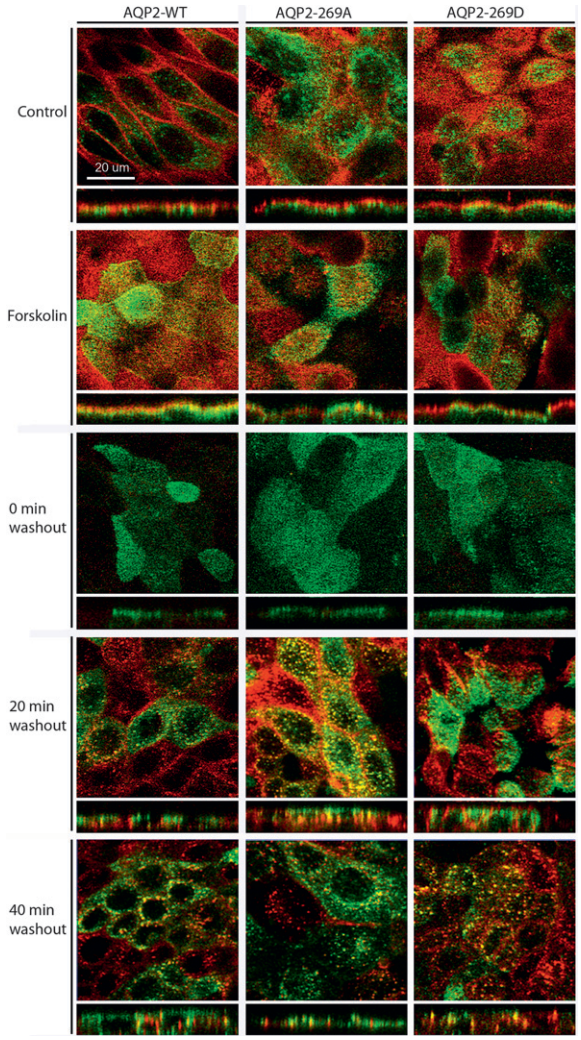

Fig. 4. Confocal laser scanning microscopy of internalization in MDCK cells expressing AQP2-WT, AQP2-269A, and AQP2-269D. AQP2 is depicted in green, biotin in red, and colocalization in yellow. Images are shown in X–Y and X–Z projections.

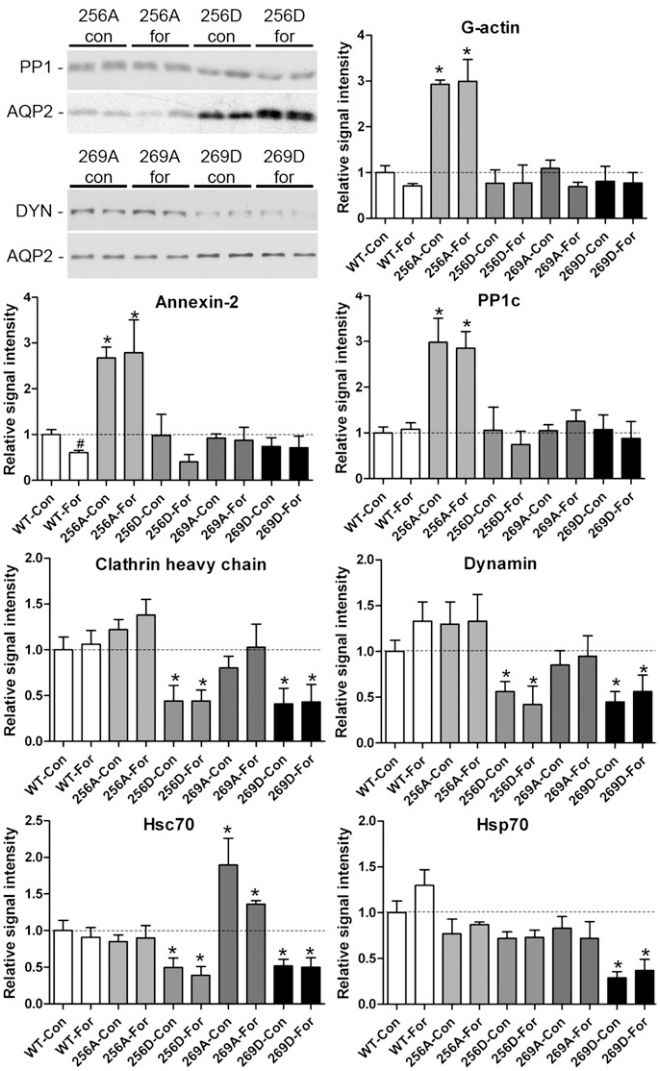

Fig. 5. Co-IP of AQP2 mutants with interacting proteins. Representative immunoblots are shown for illustrative purposes. Analysis is shown of AQP2-interacting proteins as assessed by immunoblotting. An asterisk indicates a significant difference compared to corresponding WT-AQP2 group. "#" indicates a significant difference compared to the corresponding control group within each cell line.

AQP2 trafficking or constitutive recycling (10). Previous studies demonstrate that AVP results in a rapid decrease in phosphorylation of S261 (5, 24), but current results suggest that the biological significance of phosphorylation at S261 remains undetermined. Similarly to S261, mutation of S264 to either alanine or aspartate had no significant effect on the ability of AQP2 to traffic to the plasma membrane. Taken together, we conclude that neither S261 nor S264 plays any significant role in cAMP-induced AQP2 trafficking.

Phosphorylation of AQP2 at S256 and S269 Slows AQP2 Internalization from the Plasma Membrane. Reducing the extent of AQP2 endocytosis is an alternative mechanism to increasing the total fraction of AQP2 on the plasma membrane following AVP stimulation. Indeed, an endocytosis blockade by methyl-β-cyclodextrin treatment results in accumulation of AQP2 in the membrane (22). We found that both 256D-AQP2 and 269D-AQP2 forms of AQP2 were internalized from the apical plasma membrane at a significantly slower rate than WT-AQP2. Previous studies have indicated that AQP2 can accumulate on the plasma membrane in an S256 phosphorylation-independent way (22, 25) and that, under some circumstances, internalization of AQP2 does not depend on S256 (3). This seems contradictory to our findings. However, S256 phosphorylation occurs before and is required for downstream S269 phosphorylation (7). Combined with our current findings, it is plausible that S256-mediated phosphorylation of S269 may be the main regulator of internalization. Furthermore, although the kinase that regulates S269 phosphorylation is unknown, S269 is a weak consensus site for PKG, and both nitric oxide and ANP, known to increase cGMP levels, can induce apical AQP2 accumulation (2).

The AQP2 trafficking process is made even more complicated by the sometimes underestimated role of constitutive trafficking. Several studies indicate that the constitutive recycling of AQP2 does not depend on phosphorylation at S256 (22, 26) whereas this phosphorylation is an essential step in AVP-mediated translocation of AQP2. We propose that AVP may be involved in two mechanisms to increase AQP2 membrane abundance: (*i*) AVP induces acute S256 phosphorylation, exocytosis, and subsequent S269 phosphorylation, resulting in reduced AQP2 endocytosis, and (*ii*) AVP, by stimulation of PKA activity and S269 phosphorylation in the membrane slows down the endocytic arm

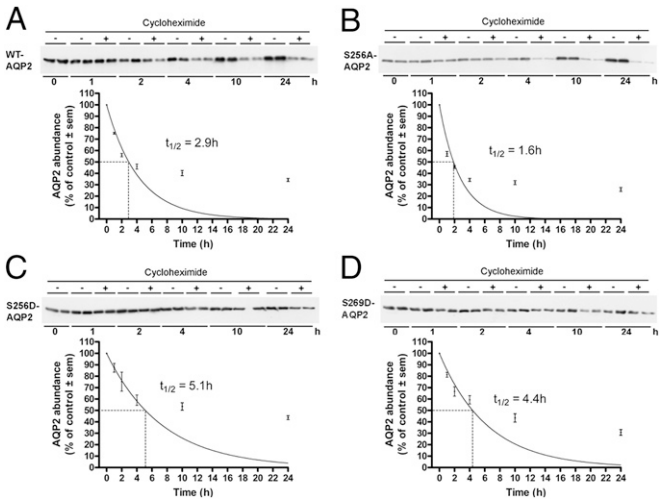

Fig. 6. Assessment of AQP2 protein half-life in MDCK cells. Representative immunoblots are shown. Average band densities for each time point were normalized to time point zero. Curves show data fitted using nonlinear regression and a one-phase exponential decay equation.

of the constitutive AQP2 recycling pathway. As recycling occurs at a high speed, the effect of AVP on constitutive recycling may contribute substantially to AQP2 membrane accumulation. In line with this hypothesis, Nunes et al. (21) suggested a more significant role of S256 in the reduction of AQP2 endocytosis in response to AVP rather than acting as an "on-switch" for exocytosis.

To find an explanation at the molecular level for the observed patterns of internalization, we performed co-IP studies. Several proteins involved in endocytosis were significantly less abundant in AQP2 pull-downs from both S256D- and 269D-AQP2–expressing cells. Endocytosis of AQP2 begins in clathrin-coated pits (27) and is a form of selective internalization. Both dynamin and clathrin heavy chain interacted less with S256D and S269D forms of AQP2, suggesting that these forms of AQP2 are less abundant in clathrin-coated vesicles. Although our co-IP studies do not demonstrate a direct interaction between these proteins and AQP2 (co-IP proteins could interact indirectly as part of a binding partner complex), it has been previously shown that blocking clathrin-mediated endocytosis causes hormone and phosphorylation-independent accumulation of AQP2 on the apical membrane (22). Furthermore, the interactions of both Hsp70 and Hsc70, which bind directly to AQP2 and participate in clathrin-mediated endocytosis (14), were reduced with S256D- and 269D-AQP2. Of course, there are technical constraints to the use of co-IP and AQP2 mutant cells. One constraint is the possibility that the mutations themselves, rather than their intended mimicking of AQP2 phosphorylation status, changes the protein–protein interactions. This has been previously suggested to be the case for Hsp70, which was found to have reduced binding to both the S256A- and S256D-AQP2 forms (14). Future studies using phosphorylated peptides and mass spectrometry, as used previously for analyzing the S256 residue of AQP2 (13), may help resolve these issues. We conclude that the reduced internalization of the S256D and S269D forms of AQP2 may be caused by reduced phosphorylation-mediated protein–protein interactions with the endocytic machinery.

In addition to proteins involved in AQP2 endocytosis, we found three proteins that interacted significantly more with nonphosphorylated S256 AQP2: annexin-2, PP1c, and γ-actin. The greater interaction of γ-actin with S256A-AQP2, along with the significantly reduced interaction with WT-AQP2 following forskolin stimulation, suggests that γ-actin is released from AQP2 following phosphorylation. Putatively, in the resting state AQP2 may be bound to γ-actin, keeping AQP2-containing vesicles out of the exocytic pathway. Elegant studies by Noda et al. have shown a similar mechanism, where AQP2 is released from globular actin in response to AVP-induced S256 phosphorylation, resulting in interaction with tropomyosin 5b, subsequent destabilization of F-actin, and AQP2 trafficking (26). PP1 may play a similar role in "negatively" regulating AQP2 function.

Phosphorylation of AQP2 Plays a Role in AQP2 Degradation. Long-term AVP exposure results in increased AQP2 abundance (28) that is usually ascribed to AVP-mediated regulation of transcription. Our data suggest that AVP-mediated phosphorylation could also regulate AQP2 abundance. The whole-cell abundance of a protein can be mediated by regulating the rate at which it is degraded, in addition to the rate at which it is synthesized. Regulated degradation has been observed for other membrane channels, e.g., epithelial Na+ channel (29). Degradation of AQP2 can occur via both lysosomal and proteasomal pathways (30). WT-AQP2 in our MDCK cells had a relatively short half-life of ≈3 h. In other cell models, the AQP2 protein half-life is also relatively short, e.g., 6 h in mpkCCD$_{c14}$ cells (30). The mutants S256D and S269D had a significantly longer half-life compared to WT-AQP2. From our studies, we cannot determine whether the decreased degradation of 256D- and 269D-AQP2 is due to their decreased internalization and subsequently reduced sorting to the proteolytic pathway or due to a more direct effect such as reduced sorting to the proteolytic pathways via reduced protein–protein interactions; e.g., LIP5 interacts with the COOH-terminal tail of AQP2 (17). In contrast, mutating S264 to either alanine or aspartate resulted in increased AQP2 protein half-life, without significant effects on protein trafficking, suggesting, as previously (6), a more direct role of this residue in sorting AQP2 following endocytic retrieval. For determination of protein half-life, we used the protein synthesis inhibitor cycloheximide. One constraint to this approach is that cycloheximide abrogrates overall protein synthesis. Thus, proteolytic proteins may themselves be degraded, leading to reduced protein degradation rates, which seems to be evident in our system at later time points. This constraint should be equal in all cell lines. Regulated proteolysis is often carried out via the ubiquitin–proteasome pathway (31). AQP2 is short chain ubiquitinated at K270, which can mediate its endocytosis, sorting to multivesicular bodies (MVBs) and degradation (4). Due to the close proximity of K270 to S269, one could speculate that the level of AQP2 ubiquitination may also be regulated by phosphorylation at the neighboring serine residue, subsequently regulating AQP2 endocytosis and/or degradation. This hypothesis requires further investigation.

Methods

See *SI Methods* for a detailed discussion of methods.

Constructs, Stable Transfection, and Cell Culture. Mutant forms of AQP2 were generated by site-directed mutagenesis, replacing serine residues of mouse AQP2 at positions 256, 261, 264, and 269 with either alanine (A), which prevents phosphorylation, or aspartic acid (D), which mimics the charged state of phosphorylated AQP2. Generation and culture of stable AQP2-expressing cell lines were as described previously (7).

Biotinylation Assay. Cells were seeded on 6-well filter plates (Costar, 0.4 μm) and grown to confluence in complete DMEM (DMEM + glutamax + 5% FCS). Cells were treated for 30 min at 37°C with pure media containing 25 μM forskolin where indicated. All observations were performed in triplicate. Cells were washed with ice-cold PBS–CM (10 mM PBS, 1 mM $CaCl_2$, 0.1 mM $MgCl_2$, pH 8) and incubated for 45 min at 4°C in ice-cold biotinylation buffer (10 mM triethanolamine, 2 mM $CaCl_2$, 125 mM NaCl, pH 7.5) containing Sulfosuccinimidyl 2-(biotinamido)-ethyl-1,3-dithiopropionate (Sulfo-NHS-SS-biotin) (1 mg/mL final concentration, Pierce) added to the apical compart-

ment. Cells were washed with ice-cold quenching buffer (PBS–CM, 50 mM Tris·HCl, pH 8) followed by two washes in PBS–CM. Cells were scraped and samples spun at 4000 × *g* for 5 min at 4°C. Cell pellets were resuspended in 500 μl of lysis buffer (150 mM NaCl, 5 mM EDTA, 50 mM Tris·HCl, pH 7.5, 1% Triton x-100, leupeptin 5 μg/mL, phefablock 100 μg/mL, phosphatase inhibitor mixture (Sigma) 10 μl/mL). A fraction of the supernatant was retained for AQP2 total protein estimates. The remaining supernatant was transferred to spin columns containing NeutrAvidin gel slurry (Pierce) and incubated for 60 min at RT with end-over-end mixing. After extensive washing, samples were eluted in elution buffer (62.53 mM Ultrapure Tris, 21.75% glycerol, 104.03 mM SDS, bromophenol blue 89.5 μM, 97.24 mM DTT in PBS 0.01 M, pH 7.2) and heated to 65°C for 10 min before immunoblot analysis. Data were obtained from three independent experiments. We performed immunoblotting of samples using an antibody recognizing the intracellular protein calmodulin to validate that biotin binds only to membrane proteins and does not cross the cell membrane (Fig. S5).

Biotin Internalization Assay. Biotinylation assay was as above. After removal of biotin solution and washing, some filters were incubated in pure media at 37°C for various time points. All observations were performed in duplicate. After reincubation, cells were washed in ice-cold PBS–CM and kept on ice. Cells were washed three times for 20 min each time in biotin stripping solution (100 mM MesNa, 100 mM NaCl, 1 mM EDTA, 50 mM Tris, pH 8.6, 0.2% BSA), and the reaction was quenched with 120 mM iodoacetic acid in PBS–CM. Cells were washed in ice-cold PBS–CM, and samples were prepared as described above before immunoblot analysis. Internalization of AQP2 was determined from three to four independent experiments by densitometry of the biotinylated signal and normalized to the signal intensity in forskolin-stimulated nonstripped samples.

Immunocytochemistry and Laser Scanning Confocal Microscopy. For trafficking studies, cells were washed two times in prewarmed media and treated for 30 min at 37°C with pure media containing 25 μM forskolin where indicated. For internalization studies, forskolin stimulation, surface biotinylation, and reincubation followed by MesNa stripping was performed as described above. A Leica TCS SL confocal microscope was used for imaging. Image stacks were taken using an HCX PL APO 40×/1.25–0.75 Oil C9 lens and a *z*-distance of 0.3 μm between images. A minimum of four independent stacks from two different experiments were analyzed using Imaris image analysis software.

Cycloheximide Studies. Cells were grown to confluence in complete DMEM. On the day of the experiment, the medium was replaced with either complete DMEM containing 50 μM cycloheximide (in DMSO) or a DMSO vehicle. Observations were performed in duplicate. Cells were incubated for various time points at 37°C and 5% CO_2. Cells were washed twice in PBS and proteins were extracted in 500 μl of lysis buffer. For calculation of the protein half-life, average band densities for each time point were normalized to controls, and data were fitted using nonlinear regression and a one-phase exponential decay equation using Graphpad Prism software. Data were obtained from three independent experiments.

Co-IP. Co-IP was performed using an anti-AQP2 antibody directed against the COOH terminus of AQP2, K5007 (7), and the Catch and Release v2.0 system (Chemicon). Antibodies used are described in Table S1. The signal intensity of each band on each immunoblot was obtained using densitometry and Quantity One 4.2.3 software. On each individual blot, the ratios of the signal intensity of binding protein over the signal intensity of AQP2 on the same blot were calculated. For each experiment, the difference in the ratio for each mutant (or different treatment) compared to WT-AQP2 was calculated ($n = 2$ observations/experiment). The change in relative signal intensity obtained from at least three experiments was analyzed.

Statistics and Data Analysis. Comparisons of data from each group were performed using one-way ANOVA followed by Tukey's multiple comparisons test. Multiple comparisons tests were applied only when a significant difference ($P < 0.05$) was determined in the ANOVA. All data are presented as mean ± SE.

ACKNOWLEDGMENTS. We thank Mark Knepper for the K5007 AQP2 antibody and Christian Westberg, Tina Dreyer, and Inger Merete Paulsen for technical assistance. Funding for R.A.F. is provided by the Danish Medical Research Council, the Novo Nordisk Foundation, the Carlsberg Foundation, and a Marie Curie Intra-European Fellowship. The Water and Salt Research Center is established and supported by the Danish National Research Foundation (Danmarks Grundforskningsfond).

1. Knepper MA, Nielsen S (1993) Kinetic model of water and urea permeability regulation by vasopressin in collecting duct. *Am J Physiol* 265:F214–F224.
2. Bouley R, *et al.* (2000) Nitric oxide and atrial natriuretic factor stimulate cGMP-dependent membrane insertion of aquaporin 2 in renal epithelial cells. *J Clin Invest* 106:1115–1126.
3. Nejsum LN, Zelenina M, Aperia A, Frøkiaer J, Nielsen S (2005) Bidirectional regulation of AQP2 trafficking and recycling: Involvement of AQP2-S256 phosphorylation. *Am J Physiol Renal Physiol* 288:F930–F938.
4. Kamsteeg EJ, *et al.* (2006) Short-chain ubiquitination mediates the regulated endocytosis of the aquaporin-2 water channel. *Proc Natl Acad Sci USA* 103: 18344–18349.
5. Hoffert JD, *et al.* (2007) Dynamics of aquaporin-2 serine-261 phosphorylation in response to short-term vasopressin treatment in collecting duct. *Am J Physiol Renal Physiol* 292:F691–F700.
6. Fenton RA, *et al.* (2008) Acute regulation of aquaporin-2 phosphorylation at Ser-264 by vasopressin. *Proc Natl Acad Sci USA* 105:3134–3139.
7. Hoffert JD, *et al.* (2008) Vasopressin-stimulated increase in phosphorylation at Ser269 potentiates plasma membrane retention of aquaporin-2. *J Biol Chem* 283: 24617–24627.
8. Fushimi K, Sasaki S, Marumo F (1997) Phosphorylation of serine 256 is required for cAMP-dependent regulatory exocytosis of the aquaporin-2 water channel. *J Biol Chem* 272:14800–14804.
9. Katsura T, Gustafson CE, Ausiello DA, Brown D (1997) Protein kinase A phosphorylation is involved in regulated exocytosis of aquaporin-2 in transfected LLC-PK1 cells. *Am J Physiol* 272:F817–F822.
10. Lu HA, *et al.* (2008) The phosphorylation state of serine 256 is dominant over that of serine 261 in the regulation of AQP2 trafficking in renal epithelial cells. *Am J Physiol Renal Physiol* 295:F290–F294.
11. Moeller HB, Knepper MA, Fenton RA (2009) Serine 269 phosphorylated aquaporin-2 is targeted to the apical membrane of collecting duct principal cells. *Kidney Int* 75: 295–303.
12. Moeller HB, MacAulay N, Knepper MA, Fenton RA (2009) Role of multiple phosphorylation sites in the COOH-terminal tail of aquaporin-2 for water transport: Evidence against channel gating. *Am J Physiol Renal Physiol* 296:F649–F657.
13. Zwang NA, *et al.* (2009) Identification of phosphorylation-dependent binding partners of aquaporin-2 using protein mass spectrometry. *J Proteome Res* 8: 1540–1554.
14. Lu HA, *et al.* (2007) Heat shock protein 70 interacts with aquaporin-2 and regulates its trafficking. *J Biol Chem* 282:28721–28732.
15. Kamsteeg EJ, *et al.* (2007) MAL decreases the internalization of the aquaporin-2 water channel. *Proc Natl Acad Sci USA* 104:16696–16701.
16. Noda Y, *et al.* (2004) Aquaporin-2 trafficking is regulated by PDZ-domain containing protein SPA-1. *FEBS Lett* 568:139–145.
17. van Balkom BW, *et al.* (2009) LIP5 interacts with aquaporin 2 and facilitates its lysosomal degradation. *J Am Soc Nephrol* 20:990–1001.
18. Noda Y, Horikawa S, Katayama Y, Sasaki S (2005) Identification of a multiprotein "motor" complex binding to water channel aquaporin-2. *Biochem Biophys Res Commun* 330:1041–1047.
19. Gerke V, Creutz CE, Moss SE (2005) Annexins: Linking Ca2+ signalling to membrane dynamics. *Nat Rev Mol Cell Biol* 6:449–461.
20. Brown D (2003) The ins and outs of aquaporin-2 trafficking. *Am J Physiol Renal Physiol* 284:F893–F901.
21. Nunes P, *et al.* (2008) A fluorimetry-based ssYFP secretion assay to monitor vasopressin-induced exocytosis in LLC-PK1 cells expressing aquaporin-2. *Am J Physiol Cell Physiol* 295:C1476–C1487.
22. Lu H, *et al.* (2004) Inhibition of endocytosis causes phosphorylation (S256)-independent plasma membrane accumulation of AQP2. *Am J Physiol Renal Physiol* 286:F233–F243.
23. van Balkom BW, *et al.* (2002) The role of putative phosphorylation sites in the targeting and shuttling of the aquaporin-2 water channel. *J Biol Chem* 277: 41473–41479.
24. Hoffert JD, Pisitkun T, Wang G, Shen RF, Knepper MA (2006) Quantitative phosphoproteomics of vasopressin-sensitive renal cells: Regulation of aquaporin-2 phosphorylation at two sites. *Proc Natl Acad Sci USA* 103:7159–7164.
25. Valenti G, *et al.* (2000) The phosphatase inhibitor okadaic acid induces AQP2 translocation independently from AQP2 phosphorylation in renal collecting duct cells. *J Cell Sci* 113:1985–1992.
26. Noda Y, *et al.* (2008) Reciprocal interaction with G-actin and tropomyosin is essential for aquaporin-2 trafficking. *J Cell Biol* 182:587–601.
27. Sun TX, *et al.* (2002) Aquaporin-2 localization in clathrin-coated pits: Inhibition of endocytosis by dominant-negative dynamin. *Am J Physiol Renal Physiol* 282: F998–F1011.
28. DiGiovanni SR, Nielsen S, Christensen EI, Knepper MA (1994) Regulation of collecting duct water channel expression by vasopressin in Brattleboro rat. *Proc Natl Acad Sci USA* 91:8984–8988.
29. Staub O, *et al.* (1997) Regulation of stability and function of the epithelial Na+ channel (ENaC) by ubiquitination. *EMBO J* 16:6325–6336.
30. Hasler U, *et al.* (2002) Long term regulation of aquaporin-2 expression in vasopressin-responsive renal collecting duct principal cells. *J Biol Chem* 277:10379–10386.
31. Acconcia F, Sigismund S, Polo S (2009) Ubiquitin in trafficking: The network at work. *Exp Cell Res* 315:1610–1618.